nature materials

LETTERS

PUBLISHED ONLINE: 30 MAY 2010 | DOI: 10.1038/NMAT2770

Tunable multifunctional topological insulators in ternary Heusler compounds

Stanislav Chadov[1], Xiaoliang Qi[2,3], Jürgen Kübler[4], Gerhard H. Fecher[1], Claudia Felser[1]* and Shou Cheng Zhang[3]*

Recently the quantum spin Hall effect was theoretically predicted and experimentally realized in quantum wells based on the binary semiconductor HgTe (refs 1–3). The quantum spin Hall state and topological insulators are new states of quantum matter interesting for both fundamental condensed-matter physics and material science[1–11]. Many Heusler compounds with $C1_b$ structure are ternary semiconductors that are structurally and electronically related to the binary semiconductors. The diversity of Heusler materials opens wide possibilities for tuning the bandgap and setting the desired band inversion by choosing compounds with appropriate hybridization strength (by the lattice parameter) and magnitude of spin–orbit coupling (by the atomic charge). Based on first-principle calculations we demonstrate that around 50 Heusler compounds show band inversion similar to that of HgTe. The topological state in these zero-gap semiconductors can be created by applying strain or by designing an appropriate quantum-well structure, similar to the case of HgTe. Many of these ternary zero-gap semiconductors (LnAuPb, LnPdBi, LnPtSb and LnPtBi) contain the rare-earth element Ln, which can realize additional properties ranging from superconductivity (for example LaPtBi; ref. 12) to magnetism (for example GdPtBi; ref. 13) and heavy fermion behaviour (for example YbPtBi; ref. 14). These properties can open new research directions in realizing the quantized anomalous Hall effect and topological superconductors.

According to their electronic structure all bulk materials are divided into metals, which have a finite electron density at the Fermi energy, and insulators, which show a bandgap. Recently, a new class of the so-called topological states has emerged—the quantum spin Hall (QSH) state in two dimensions and its generalization in three dimensions. The corresponding materials, called topological insulators (TIs), have been predicted theoretically and recently studied experimentally[1,2,8–11]. The TI is a new state of quantum matter with a full insulating gap in the bulk, but with topologically protected gapless surface or edge states on the boundary. Research on TIs has attracted considerable attention owing to both a fundamental interest in a new state of matter and its possible application in new spintronic devices[4]. All the TIs discovered so far were either alloys ($Bi_{1-x}Sb_x$; refs 7,8) or binary compounds (HgTe; refs 1,2, Bi_2Se_3, Sb_2Te_3 and Bi_2Te_3; refs 9–11). This Letter reports on tunable multifunctional TIs within the class of ternary semiconducting Heusler compounds. The great diversity of these materials compared with binary compounds (more than 200 semiconductors among 500 Heusler compounds) opens wide possibilities for tuning their band structure and enables an effective search for the optimal TI material for applications.

In particular, several compounds, YPtSb, YPdBi and ScAuPb, are found at their experimental lattice constants[15] close to the border between the trivial and topological insulators, with all relevant bands degenerate at the centre of the Brillouin zone, the Γ point. Such a material can be easily transformed from a trivial to a topological insulator and vice versa by a small variation of the lattice constant (by applying pressure or growing films on an appropriate substrate). Many TI candidate compounds (LnAuPb, LnPdBi, LnPtSb and LnPtBi) containing rare-earth elements Ln with strongly correlated f electrons can exhibit various conventional orders, such as magnetism[13], superconductivity or heavy fermion behaviour[14]. Such conventional orders in TIs enable the realization of many new topological effects and exotic particles, such as the image monopole effect[16], axions[17] and Majorana fermions[18]. Thus the ternary TIs are multifunctional and can be exploited to design new devices. Combinations of the ternary trivial–topological insulators (such as ScPtSb–ScPtBi, similar to CdTe–HgTe) can be used as quantum-well devices for the QSH systems.

Ternary Heusler compounds of X_2YZ or XYZ composition (with X, Y the transition or rare-earth metals and Z the main-group element) form a class of materials that are well suited for various spintronic applications[19]. The semiconducting nature of these compounds arises owing to the strong tendency towards covalent bonding. From basic structural and bonding considerations, the X_2YZ Heusler compounds ($L2_1$ structure) with 18 or 24 valence electrons[20] and XYZ Heuslers ($C1_b$) with 18 valence electrons[21–23] are expected to exhibit a gap at the Fermi energy. In the following we shall focus on the XYZ Heuslers (also called half-Heuslers). The relation to the classical semiconductors is easy to understand for such materials as, for example, LiZnAs. More surprisingly, LaPtBi (sometimes also named LaBiPt) is a semiconductor formed by three metallic elements. Typically, the XYZ half-Heuslers can be viewed as consisting of an X^{n+} ion 'stuffing' the zinc-blende YZ^{n-} sublattice (here Li^+ stuffed in $[ZnAs]^-$ or La^{3+} stuffed in a $[PtBi]^{3-}$ sublattice), where the number of valence electrons associated with YZ^{n-} is equal to 18 ($d^{10}+s^2+p^6$). Eighteen-electron compounds are closed-shell species, non-magnetic and semiconducting.

Figure 1 illustrates a comparison of the zinc-blende and the Heusler structures. The additional stuffed rare-earth atoms are shown as orange spheres. Similar to the binary semiconductors, the bandgap can be tuned by the electronegativity difference of the constituents and the lattice constant[23] in a wide range from about 4 eV (LiMgN) down to zero (LaPtBi). The semiconducting Fe_2VAl

[1]Institut für Anorganische Chemie und Analytische Chemie, Johannes Gutenberg-Universtität, 55099 Mainz, Germany, [2]Microsoft Research, Station Q, Elings Hall, University of California, Santa Barbara, California 93106, USA, [3]Department of Physics, McCullough Building, Stanford University, Stanford, California 94305-4045, USA, [4]Institut für Festkörperphysik, Technische Universität Darmstadt, 64289 Darmstadt, Germany.
*e-mail: felser@uni-mainz.de; sczhang@stanford.edu.

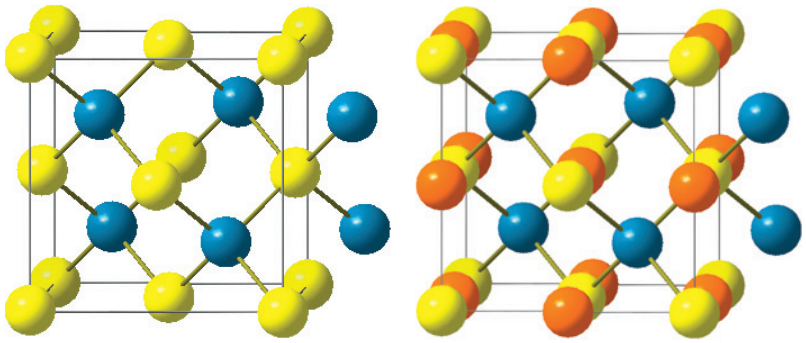

Figure 1 | Comparison of the zinc-blende and the $C1_b$ crystal structure. The zinc-blende (XY) structure is shown on the left, and the $C1_b$ (XYZ) on the right. Yellow and blue spheres correspond to the main-group (Z) and transition (Y) elements, respectively. The orange spheres in $C1_b$ stand for the additional stuffing (X) element.

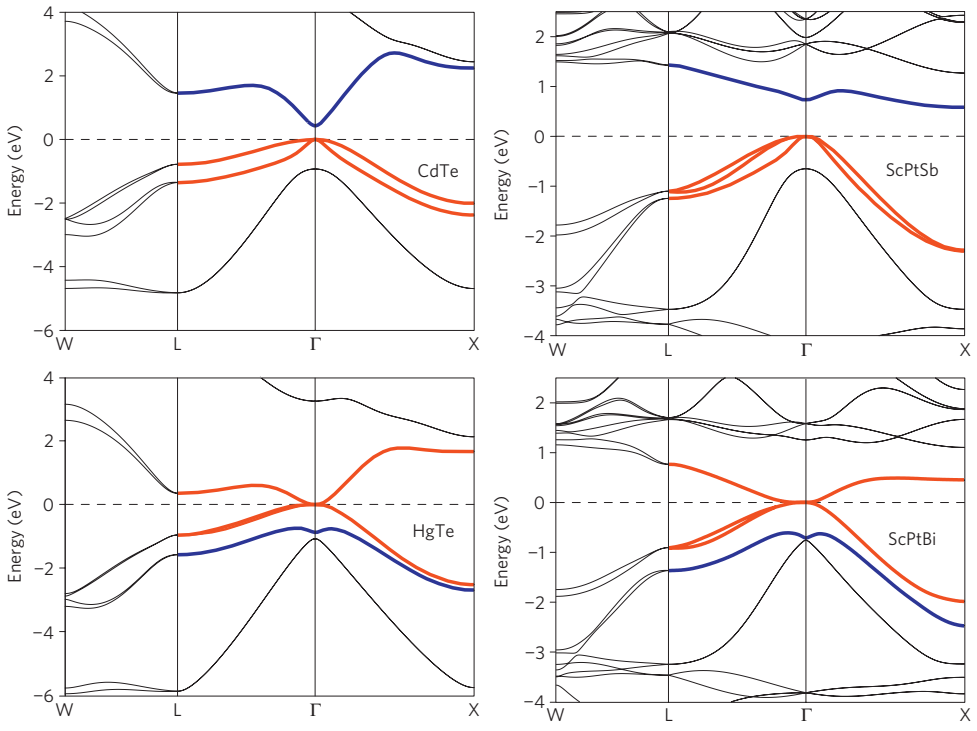

Figure 2 | Bandstructures of CdTe and HgTe compared with ScPtSb and ScPtBi Heuslers. Red colour marks the bands with Γ_8 symmetry, blue with Γ_6. Comparison reveals obvious similarity between binary systems and their ternary equivalents: both CdTe and ScPtSb are trivial semiconductors with Γ_6 situated above Γ_8, which sits at the Fermi energy (set to zero). Both HgTe and ScPtBi are topological with inverted band order; the band with Γ_6 symmetry is situated below Γ_8.

and ZrNiSn (ref. 24) Heusler compounds in addition demonstrate excellent thermoelectric properties, just like the known TIs Bi_2Te_3 and Bi_2Se_3[25,26]. To understand ternary compounds as TIs, we compare them with the binary compounds studied in the literature. For example, CdTe is a trivial semiconductor, whereas HgTe is a topological system[1–3,7]. Such a drastic change in properties occurs owing to an interplay of the spin–orbit coupling (produced by the heavy Hg and Te atoms) and the degree of hybridization (controlled by the lattice constant). The same considerations apply to all ternary semiconducting Heusler compounds. We verify this by means of first-principle band-structure calculations by using the fully relativistic version (A. Perlov, A. Yaresko, V. Antonov, Spin-polarized relativistic linear muffin-tin orbitals package for electronic structure calculations, PY-LMTO, unpublished) of the standard linearized muffin-tin orbitals approach. The exchange–correlation part of the effective potential was treated using the Vosko–Wilk–Nusair parameterization[27] of the local-density approximation. The example in Fig. 2 compares the calculated band structures of CdTe and HgTe with those of ScPtSb and ScPtBi. For direct comparison with model calculations[1], we mark the relevant bands possessing Γ_6 symmetry as blue and Γ_8 as red. The band structures of these ternary compounds reveal clear fingerprints: on the one hand both CdTe and ScPtSb exhibit a direct gap at the Γ point between the conduction (blue) and the valence (red) bands of Γ_6 and Γ_8 symmetries, respectively. On the other hand, the band structures of HgTe and ScPtBi exhibit the same band inversion: Γ_6 (blue) is now situated below Γ_8 (red), which remains at the Fermi energy. This is the necessary condition for the TI state, because it changes the parity of the wavefunction compared with CdTe or ScPtSb (for details see the work of Dai and co-workers[3]).

To illustrate the impressive number of new topological compounds and the possibility to tune the Γ_6–Γ_8 band ordering in this class of materials, we have carried out similar calculations for all relevant Heuslers containing Sc, Y, La, Lu and Th. The energy

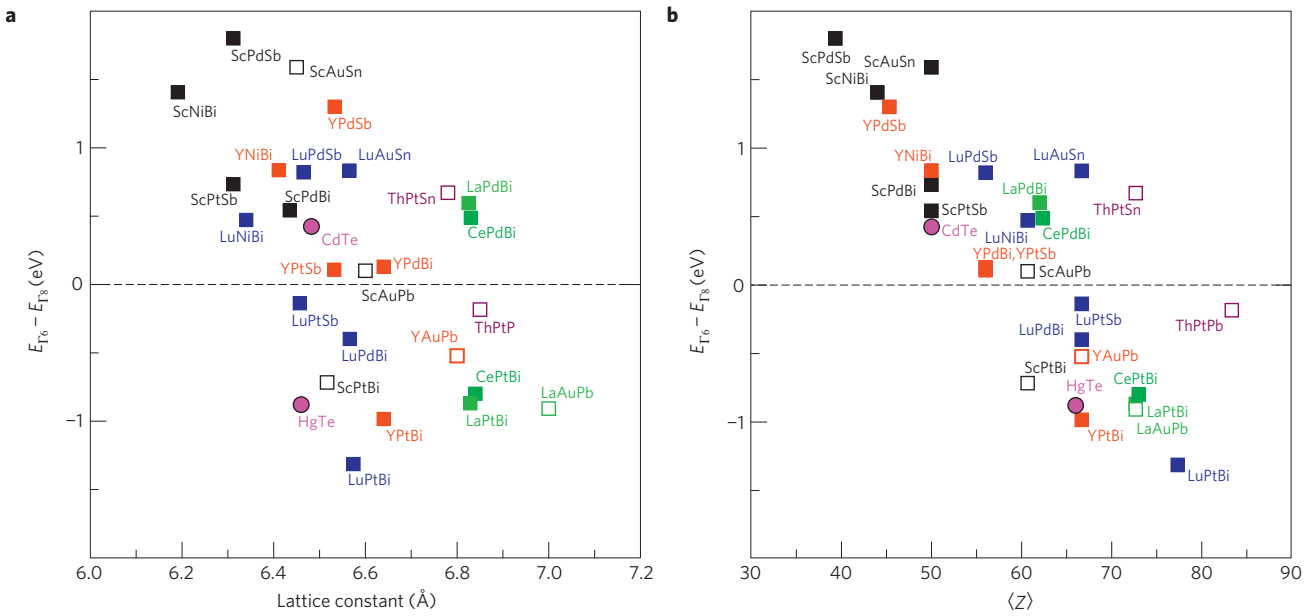

Figure 3 | $E_{\Gamma_6} - E_{\Gamma_8}$ difference calculated for various Heuslers at their experimental lattice constants. HgTe and CdTe binaries are shown for comparison. Open squares mark the systems not reported in the literature. **a**, $E_{\Gamma_6} - E_{\Gamma_8}$ difference as a function of the lattice constant. Pairs of materials with well-matching lattices for the QSH quantum wells can be easily picked up along the same vertical lines. The borderline compounds (between trivial and topological) insulators (YPtSb, YPdBi, ScAuPb) are situated closer to the zero horizontal line. **b**, $E_{\Gamma_6} - E_{\Gamma_8}$ difference as a function of the average spin–orbit coupling strength represented by the average nuclear charge $\langle Z \rangle = (1/N)\sum_{i=1}^{N} Z(X_i)$, where N is 3 for ternaries and 2 for binaries.

difference between Γ_6 and Γ_8 bands as a function of lattice constant is shown in Fig. 3a. Each subgroup (for example, Ln = Sc, Y, La, Lu) is marked by a certain colour. Compounds containing f electrons, such as Pr, Tb and so on (except for Ce), are not presented here, because their partially filled f-electron shells with strong correlations require special treatment that goes beyond the standard local-density approximation approach. The compounds with $E_{\Gamma_6} - E_{\Gamma_8} > 0$ are trivial insulators, whereas those with $E_{\Gamma_6} - E_{\Gamma_8} < 0$ are the TI candidates. The latter group consists of zero-gap semiconductors with a doubly degenerate Γ_8 point at the Fermi energy. It follows that all existing Heuslers with zero bandgap at the Fermi energy (around 50 compounds including those based on rare earths) under certain conditions will reveal the same type of band inversion as does HgTe. Indeed, the increase of the lattice constant reduces the hybridization and closes the non-zero bandgap. Combined with sufficiently strong spin–orbit coupling it leads to a pronounced Γ_6–Γ_8 band inversion, which is the key to realize the TI state.

Figure 3b demonstrates the Γ_6–Γ_8 difference as a function of the average spin–orbit coupling expressed by the average nuclear charge over the atoms in the unit cell, that is, by $\langle Z \rangle = (1/N)\sum_{i=1}^{N} Z(X_i)$, where N is 2 for binaries and 3 for ternaries. This seems to be a suitable order parameter, which sorts the materials almost along a straight line. As follows from Fig. 3, the combinations of Pt with Bi in LnPtBi or Au with Pb in the LnAuPb series always lead to the inverted band structure. There is an additional advantage of Heusler materials which also follows from Fig. 3a: owing to the large number of compounds with different gap values it is easy to construct a quantum well consisting of the trivial and topological parts with well-matching lattice constants, similar to the HgTe–CdTe quantum well. The appropriate pairs can be chosen from the candidates situated in the middle area of Fig. 3a along the same vertical line, because the transition from trivial to topological behaviour as a function of lattice constant seems to be fairly smooth on average. The relevant combinations, for example, are ScPdBi–ScPtBi, YPdSb–YPtSb and LuAuSn–LuPtBi.

Although the analogy with HgTe is clear and convincing, we should like to demonstrate the topological non-trivial nature of the zero-gap Heuslers in a more rigorous way. Owing to the lack of inversion symmetry of the zinc-blende crystal structure, the parity criteria of ref. 7 do not apply. In this case, a simple way to determine the topological invariant is by driving the system to a known trivial system by tuning some physical parameter. For a topological non-trivial system, there must be a topological phase transition between it and the trivial system (as long as time-reversal symmetry is preserved), described by a massless Dirac theory in the bulk. This is the three-dimensional analogue of the approach in ref. 1 for the two-dimensional HgTe quantum well. For this purpose, we study the topological phase transition between trivial and inverted phases in YPdBi, one of the materials that sits right at the border between the trivial and topological insulator states (see Fig. 3). The transition between inverted and trivial phases can be tuned by a small variation of lattice constant, as shown in Fig. 4a. The insets show the corresponding band structures. At the equilibrium lattice constant a linear dispersing Dirac cone is formed by the Γ_8 light-hole and Γ_6 bands, degenerate with the Γ_8 quadratic heavy-hole band. A small variation of the lattice constant (by about $\pm 0.3\%$) substantially influences the band structure near the Fermi energy: the compression leads to a trivial state with the bandgap $E_{\Gamma_6} - E_{\Gamma_8} \approx 0.07$ eV, whereas the expansion leads to a zero-gap inverted state with a difference $E_{\Gamma_6} - E_{\Gamma_8} \approx -0.07$ eV. An analogous effect is achieved by scaling the spin–orbit coupling magnitude λ at the critical lattice constant (Fig. 4b). Suppression of spin–orbit coupling ($\lambda < 1$) drives the system into a trivial state whereas an increase ($\lambda > 1$) leads to a topological insulator.

Furthermore, for HgTe it has been proposed that a uniaxial strain can lift the degeneracy between light-hole and heavy-hole subbands of Γ_8 symmetry, which drives this zero-gap semiconductor into a real TI phase[3,7]. Similar effects can be studied by our *ab initio* calculations in Heusler compounds. Figure 5 shows the YPdBi band structure calculated for a small tetragonal strain applied along the [001] direction reducing the c/a ratio by 3%. One can see that both normal (Fig. 5a) and inverted (Fig. 5c) systems are gapped. The gapless Dirac cone at the 'critical' lattice constant (Fig. 5b) remains robust, and the quadratic heavy-hole

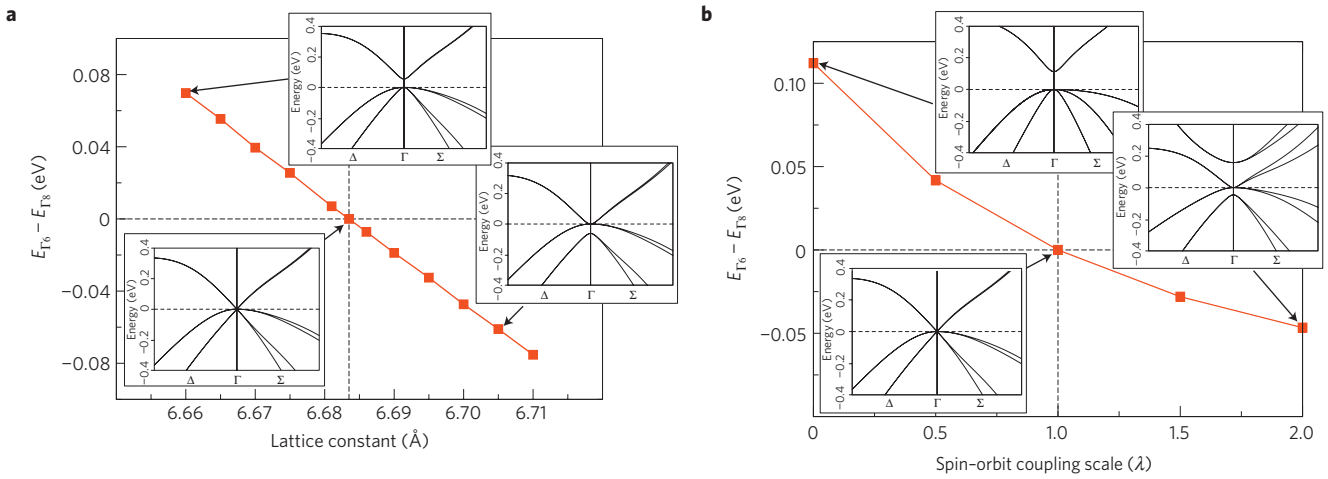

Figure 4 | $E_{\Gamma_6} - E_{\Gamma_8}$ difference for YPdBi. The insets show the band structures at the marked points along Δ and Σ symmetry directions of the Brillouin zone. **a**, $E_{\Gamma_6} - E_{\Gamma_8}$ changes on scaling the lattice constant from positive (trivial insulator) to negative (topological insulator). The borderline (critical) lattice constant (marked by a dashed vertical line) corresponds to the zero gap with a Dirac cone at the Fermi energy. **b**, Analogously, by scaling the spin–orbit coupling at the critical lattice constant, the system can be transformed from trivial ($\lambda < 1$) to topological ($\lambda > 1$).

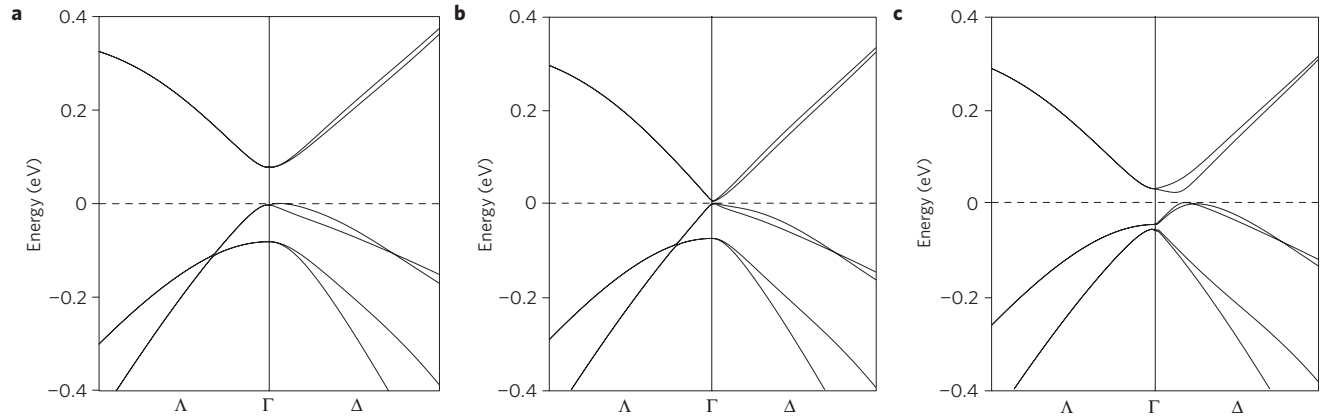

Figure 5 | Bandstructure of YPdBi under tetragonal strain ($c/a = 0.97$). **a**–**c**, At the critical lattice constant (**b**) the strain shifts down the heavy-hole band with parabolic dispersion, leaving the single Dirac cone at the Fermi energy. This effect is especially pronounced along the Λ direction, parallel to the strain. We note that along Δ (perpendicular to the strain) the bands at the Fermi energy still have a linear dispersion near the Γ point, although on a much smaller scale. Variation of the lattice constant (by ±4%) around the critical value leads to the trivial state by compression (**a**) or the topological state by expansion (**c**).

band is pushed away from the Fermi level. It should be noticed that the dispersion at the critical point is linear along all directions in momentum space around Γ, although the linear region is very small along the directions perpendicular to the strain direction. Consequently, such a transition driven by the change of lattice constant corresponds to the sign change of the mass term in the three-dimensional Dirac equation, which is exactly the theory of the topological phase transition between trivial and topological insulators. Thus we conclude that the inverted half-Heuslers are Z_2-topological non-trivial.

The proposed materials can be tuned from a trivial to a topological insulator mainly in two different ways: (1) by variation of the lattice constant (applying pressure or growing the material on appropriate substrate); and (2) by substitution of elements (varying their electronegativities or the strength of spin–orbit coupling). The devices allow for further options to manipulate the electronic structure, such as to switch the borderline compound from trivial to topological by applying a gate voltage or by constructing a quantum-well structure.

After the initial discovery of the QSH systems, the current research is now focused on the proximity effect between the TIs and other forms of ordered states, such as magnetism and superconductivity[4]. However, the TIs that we known at present only become magnetic or superconducting when doped with extrinsic elements such as Mn, Fe and Cu. In contrast, the TIs based on Heusler compounds that naturally include the *f*-shell rare-earth elements intrinsically form a stoichiometric system. Besides the chemical functions (passing of the three electrons to the zinc-blende lattice and determining the lattice size), the additional open *f*-shell element renders multifunctionality by providing the coexistence of conventional ordering with the TI state, which is necessary for the realization of new topological effects and new extended applications. Here we list several examples of such multifunctional materials. (1) Bulk magnetism found in LnPtBi (Ln = Nd, Sm, Gd, Tb, Dy; ref. 13) may realize the dynamical axion[17], which is the spin-wave excitation topologically coupled with an electromagnetic field. Such an effect provides a new design of a tunable optical modulator. (2) The heavy-fermion behaviour in YbPtBi (ref. 14) may realize the recently proposed topological Kondo insulator[28]. (3) The superconductivity in the non-centrosymmetric low-carrier LaPtBi system[12]; here, the absence of inversion symmetry is theoretically proposed to support

topological superconductivity[29]. Thus it is interesting to investigate whether the superconductivity in LaPtBi is topological.

Received 26 February 2010; accepted 20 April 2010; published online 30 May 2010

References

1. Bernevig, B. A., Hughes, T. L. & Zhang, S. C. Quantum spin Hall effect and topological phase transition in HgTe quantum wells. *Science* **314,** 1757–1761 (2006).
2. König, M. *et al.* Quantum spin Hall insulator state in HgTe quantum wells. *Science* **318,** 766–770 (2007).
3. Dai, X. *et al.* Helical edge and surface states in HgTe quantum wells and bulk insulators. *Phys. Rev. B* **77,** 125319 (2008).
4. Qi, X-L. & Zhang, S-C. The quantum spin Hall effect and topological insulators. *Phys. Today* **63,** 33–38 (2010).
5. Kane, C. L. & Mele, E. J. Quantum spin Hall effect in graphene. *Phys. Rev. Lett.* **95,** 226801 (2005).
6. Bernevig, B. A. & Zhang, S. C. Quantum spin Hall effect. *Phys. Rev. Lett.* **96,** 106802 (2006).
7. Fu, L. & Kane, C. L. Topological insulators with inversion symmetry. *Phys. Rev. B* **76,** 045302 (2007).
8. Hsieh, D. *et al.* A topological Dirac insulator in a quantum spin Hall phase. *Nature* **452,** 970–974 (2008).
9. Zhang, H. *et al.* Topological insulators in Bi_2Se_3, Bi_2Te_3 and Sb_2Te_3 with a single Dirac cone on the surface. *Nature Phys.* **5,** 438–442 (2009).
10. Xia, Y. *et al.* Observation of a large-gap topological-insulator class with a single Dirac cone on the surface. *Nature Phys.* **5,** 398–402 (2009).
11. Chen, Y. L. *et al.* Experimental realization of a three-dimensional topological insulator, Bi_2Te_3. *Science* **325,** 178–181 (2009).
12. Goll, G. *et al.* Thermodynamic and transport properties of the noncentrosymmetric superconductor LaBiPt. *Physica B* **403,** 1065–1067 (2008).
13. Canfield, P. C. *et al.* Magnetism and heavy fermion-like behavior in the RBiPt series. *J. Appl. Phys.* **70,** 5800–5802 (1991).
14. Fisk, Z. *et al.* Massive electron state in YbBiPt. *Phys. Rev. Lett.* **67,** 3310–3313 (1991).
15. Villars, P. & Calvert, L. D. *Pearson's Handbook of Crystallographic Data for Intermetallic Phases* (Amer Soc Metals, 1991).
16. Qi, X-L., Li, R., Zang, J. & Zhang, S-C. Inducing a magnetic monopole with topological surface states. *Science* **323,** 1184–1187 (2009).
17. Li, R., Wang, J., Qi, X-L. & Zhang, S-C. Dynamical axion field in topological magnetic insulators. *Nature Phys.* **6,** 284–288 (2010).
18. Fu, L. & Kane, C. L. Superconducting proximity effect and Majorana fermions at the surface of a topological insulator. *Phys. Rev. Lett.* **100,** 096407 (2008).
19. Felser, C., Fecher, G. H. & Balke, B. Spintronics: A challenge for materials science and solid-state chemistry. *Angew. Chem. Int. Ed.* **46,** 668–699 (2007).
20. Galanakis, I., Dederichs, P. H. & Papanikolaou, N. Slater–Pauling behavior and origin of the half-metallicity of the full-Heusler alloys. *Phys. Rev. B* **66,** 174429 (2002).
21. Jung, D., Koo, H. J. & Whangbo, M. H. Study of the 18-electron band gap and ferromagnetism in semi-Heusler compounds by non-spin-polarized electronic band structure calculations. *J. Mol. Struct. Theochem.* **527,** 113–119 (2000).
22. Galanakis, I., Dederichs, P. H. & Papanikolaou, N. Origin and properties of the gap in the half-ferromagnetic Heusler alloys. *Phys. Rev. B* **66,** 134428 (2002).
23. Kandpal, H. C., Felser, C. & Seshadri, R. Covalent bonding and the nature of band gaps in some half-Heusler compounds. *J. Phys. D* **39,** 776–785 (2006).
24. Sakurada, S. & Shutoh, N. Effect of Ti substitution on the thermoelectric properties of (Zr, Hf)NiSn half-Heusler compounds. *Appl. Phys. Lett.* **86,** 082105 (2005).
25. von Middendorff, A., Kohler, H. & Landwehr, G. Thermoelectric power of n-type Bi_2Se_3 in strong transverse magnetic-fields. *Phys. Status Solidi B* **57,** 203–210 (1973).
26. Hor, Y. S. *et al.* p-type Bi_2Se_8 for topological insulator and low-temperature thermoelectric application. *Phys. Rev. B* **79,** 195208 (2009).
27. Vosko, S. H., Wilk, L. & Nusair, M. Accurate spin-dependent electron liquid correlation energies for local spin density calculations: A critical analysis. *Can. J. Phys.* **58,** 1200–1211 (1980).
28. Dzero, M., Sun, K., Galitski, V. & Coleman, P. Topological Kondo insulators. *Phys. Rev. Lett.* **104,** 106408 (2010).
29. Qi, X. L., Hughes, T. & Zhang, S. C. Topological invariants for the Fermi surface of a time-reversal-invariant superconductor. *Phys. Rev. B* **81,** 134508 (2010).

Acknowledgements

We acknowledge C. X. Liu for discussion. This work is supported by ARO, grant number W911NF-09-1-0508. Financial support by the Deutsche Forschungsgemeinschaft (DFG, research unit FOR 559, project P 07) is gratefully acknowledged.

Author contributions

All authors contributed equally to the work presented in this Letter.

Additional information

The authors declare no competing financial interests. Reprints and permissions information is available online at http://npg.nature.com/reprintsandpermissions. Correspondence and requests for materials should be addressed to C.F. or S.C.Z.